Clays and Clay Minerals, Vol. 39, No. 5, 478–489, 1991.

^{57}Fe MÖSSBAUER SPECTROSCOPIC STUDY OF STRUCTURAL CHANGES DURING DEHYDRATION OF NONTRONITE: EFFECT OF DIFFERENT EXCHANGEABLE CATIONS

VITTORIO LUCA[1]

Chemistry Department, Victoria University of Wellington, P.O. Box 600
Wellington, New Zealand

Abstract—Dehydration-induced migration of different exchangeable cations toward the layers of nontronite has been studied by Mössbauer spectroscopy. As interlayer water is removed exchangeable cations migrate toward Fe^{3+} sites in the tetrahedral sheets of the nontronite ($^{IV}Fe^{3+}$) causing them to distort. The amount of distortion is linearly related to the ionic potential (IP) of the exchangeable cations and is greatest for cations with highest IP. Octahedral Fe^{3+} sites ($^{VI}Fe^{3+}$) are also affected by migration of cations into the pseudohexagonal cavities. As exchangeable cations move into the pseudohexagonal cavities, interaction with $^{VI}Fe^{3+}$ sites increases. The intensity of the outer $^{VI}Fe^{3+}$ Mössbauer doublet increases with respect to the inner $^{VI}Fe^{3+}$ doublet as the IP of the exchangeable cation increases. It appears that the exchangeable cations play a significant role in determining the thermal stability of nontronite.

Key Words—Mössbauer, Dehydration, Nontronite, Cation migration, Tetrahedral site.

INTRODUCTION

Nontronites are best regarded as Fe-rich beidellites in the sense that layer charge is of tetrahedral origin, and can result from both Al^{3+} and Fe^{3+} substitution for Si^{4+}. Suquet *et al.* (1987) have verified the beidellitic character of nontronites by utilizing the Hofmann-Klemen effect. However, their nontronite samples did not display properties typical of 2:1 Mg- or Al-smectites that have substantial tetrahedral substitution, i.e., beidellite and saponite. The features discussed by Suquet *et al.* (1987) are 1. the ability to form homogeneous hydration domains, 2. water desorption isotherms with plateaus, and 3. ordered or semiordered structures. With respect to these features, nontronite behaved similarly to montmorillonite and hectorite, which have their layer charge originating predominantly in the octahedral sheet. To explain the similar behavior of hectorite, montmorillonite, and nontronite, Suquet *et al.* (1987) postulated that, although the layer charge originates in different sites in these smectites, the charge at the layer surfaces is distributed similarly. Because of the similar layer charge distribution in nontronite, montmorillonite, and hectorite, the interaction of exchangeable cations with the layer surfaces and interlayer water was considered to be similar in the three smectites.

Nontronite also displays other unique thermal properties, such as dehydroxylation at about 200°C less than the temperature at which montmorillonite and beidellite generally dehydroxylate. Brigatti (1983) showed that the dehydroxylation temperature of nontronite correlates positively with Fe content, which in turn correlates with the unit cell *b*-dimension.

Recently Luca and Cardile (1989) reported Mössbauer spectra of Ca^{2+}-exchanged Washington nontronite (SWa-1) in various hydration states, and showed that movement of the exchangeable cations toward the nontronite layers during dehydration resulted in modification of the spectra. Specifically, for samples containing no interlayer water, a distinct shoulder formed at about −0.5 mm/s. To computer-fit these spectra adequately a three-doublet model (i.e., one $^{IV}Fe^{3+}$ doublet and two $^{VI}Fe^{3+}$ doublets) had to be used. The shoulder apparently resulted from a large increase in the quadrupole splitting (QS) of the $^{IV}Fe^{3+}$ doublet with respect to that of the hydrated sample. It was hypothesized that these $^{IV}Fe^{3+}$ sites were in the tetrahedral sheet of the nontronite. Less dramatic changes were also noted in the Mössbauer parameters of the doublets assigned to $^{VI}Fe^{3+}$ sites on dehydration. The hypothesis that the $^{IV}Fe^{3+}$ doublet fitted to the Mössbauer spectrum of the dehydrated Ca^{2+}-nontronite is Fe^{3+} in the tetrahedral sheet of the nontronite was supported by subsequent work (Luca, 1991).

The above findings raise the possibility that the dehydration of nontronite is at least in part influenced by the migration of exchangeable cations. Inasmuch as Mössbauer spectroscopy appears capable of yielding information on the modulation of the nontronite structure during migration of exchangeable cations, the dehydration of nontronite samples containing a range of exchangeable cations has been investigated by this technique.

EXPERIMENTAL

The <2-μm fraction of Washington nontronite (SWa-1) obtained from the Clay Minerals Repository of The Clay Minerals Society was separated by gravity sedi-

[1] Present address: Department of Chemistry, University of Houston, Houston, Texas 77204.

Copyright © 1991, The Clay Minerals Society

https://doi.org/10.1346/CCMN.1991.0390503 Published online by Cambridge University Press

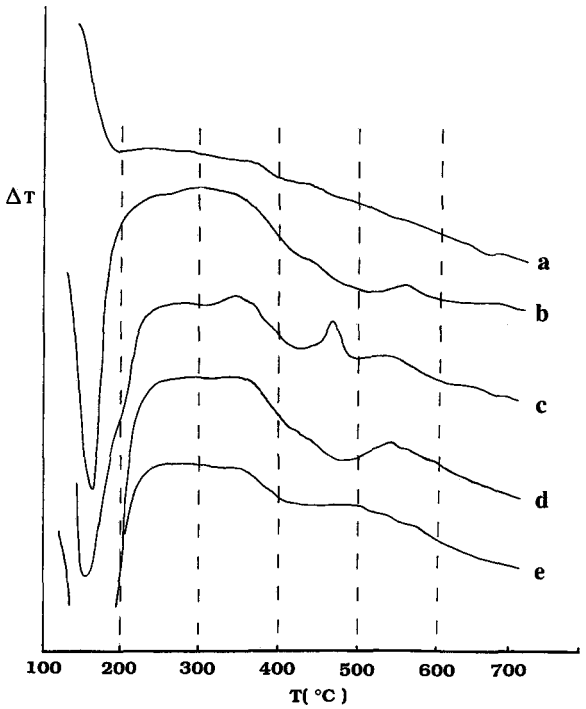


Figure 1. Differential thermal analysis curves of nontronite samples containing different exchangeable cations (a) blank (i.e., empty cell), (b) K^+-nontronite, (c) Li^+-nontronite, (d) Ca^{2+}-nontronite, and (e) Al^{3+}-nontronite.

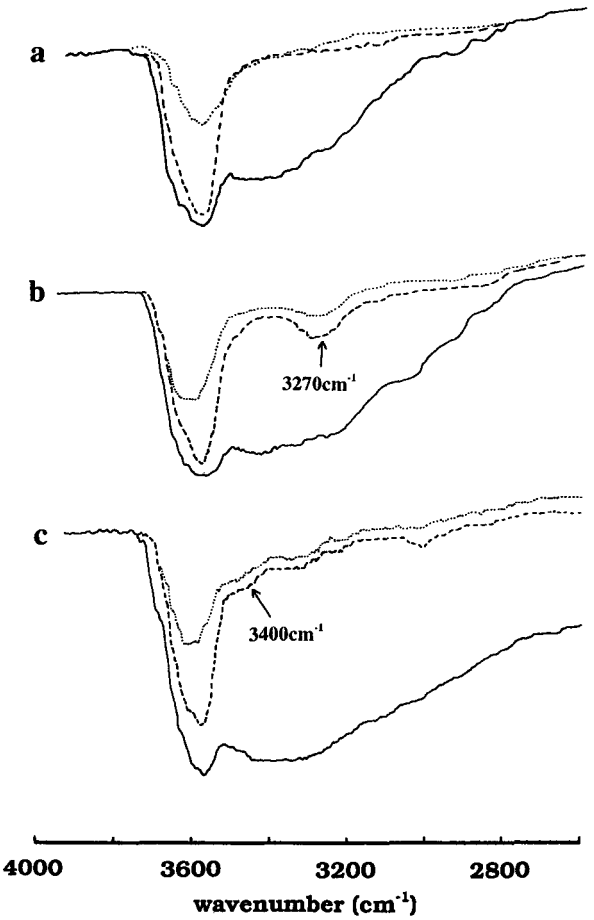


Figure 2. Infrared spectra in the 3000–4000 cm^{-1} region of nontronite containing different exchangeable cations (a) K^+-nontronite, (b) Li^+-nontronite, and (c) Al^{3+}-nontronite at ambient humidity (solid line), after heating at 200°C (dashed line), and after heating at 300°C (dotted line).

mentation and converted to the desired exchange form by stirring 1 g of the smectite with 100 ml of 1 M solutions of the desired metal chloride salt for 24 hr. The nontronite particles were separated by centrifugation and treated with a further portion of salt solution. This process was repeated three times and then the clay suspension was dialyzed to remove excess ions. To avoid the precipitation of iron oxide/hydroxides, the method of Badran *et al.* (1977) was used to exchange Fe^{3+}

No special precautions were taken to avoid the formation of interlayer polymeric hydroxy species during the preparation of the Al^{3+}-nontronite. This possibility can be excluded, however, because the d(001) value changed from 15 Å to 12.5 Å after equilibration at 0% relative humidity (RH). If hydroxy interlayers had formed, a reduction in d(001) would not be expected under such mild dehydration (Brindley and Kao, 1980). The Fe^{3+}-exchanged sample behaved similarly.

Differential thermal analyses were made in flowing nitrogen gas on a Stanton Redcroft TG770 system. Infrared spectra were recorded on a Perkin-Elmer 599B spectrometer. Thin films of nontronite samples were placed in an infrared cell in which the film could be heated under vacuum in one part of the cell and the infrared spectrum of the sample recorded in another part. The cell was fitted with NaCl windows.

Room-temperature (RT) Mössbauer spectra were recorded in 512 channels of a Cryophysics MS-102 spectrometer using a $^{57}Co/Rh$ source. The velocity was calibrated with reference to elemental iron. Spectra were computer fitted using a DECUS 11-720 Mössbauer curve-fitting program. Powdered nontronite samples (5–10 mg/cm^2) were placed into piston-design Perspex sample holders, and these were sealed with high-vacuum grease to prevent a change of hydration state.

To achieve the desired hydration state, samples were either equilibrated at the appropriate RH using saturated-salt solutions or heated in an oven at 200 or 300°C. In all experiments the hydration state was checked after acquisition of the Mössbauer spectrum by measuring the position of the basal reflection by X-ray powder diffraction (XRD). The design of the Mössbauer sample holders that were used to exclude water precluded orientation of the samples at the "magic angle" in order to avoid preferred orientation effects.

https://doi.org/10.1346/CCMN.1991.0390503 Published online by Cambridge University Press

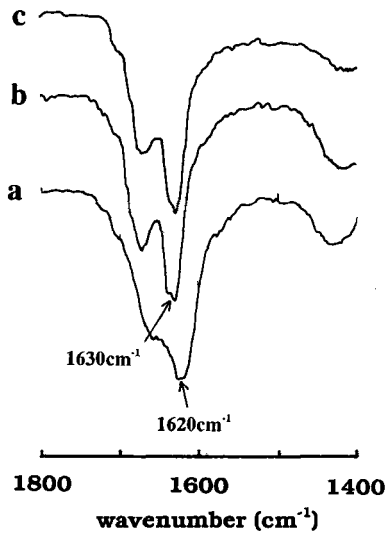


Figure 3. Infrared spectra in the 1400–1800 cm^{-1} region of Li^+-nontronite at (a) ambient humidity, (b) after heating at 200°C, and (c) after heating at 300°C.

Goodman *et al.* (1976) and Cardile (1985) demonstrated, however, that such effects are not significant for <2-μm particles of nontronite.

X-ray diffraction patterns were recorded on a Philips diffractometer equipped with a curved-crystal monochrometer and using Ni-filtered CuKα radiation.

RESULTS

Differential thermal analysis (DTA)

DTA curves of selected cation-exchanged nontronite samples are shown in Figure 1. Nontronites exchanged with K^+, Ca^{2+}, and Al^{3+} cations gave similar DTA curves. These curves consisted of one very intense endotherm at about 150°C due to the removal of adsorbed water, and a diffuse endotherm centered at about 450°C due to dehydroxylation. The peak maximum for the dehydroxylation endotherm shifted to lower temperature as the ionic potential of the exchangeable cations increased. The dehydroxylation peak maximum was at about 510°C for the K^+-nontronite, 475°C for the Ca^{2+}-nontronite, and 410°C for the Al^{3+}-nontronite sample.

The DTA curve of Li^+-nontronite had two endothermic peaks at 424 and 492°C. The possible reactions giving rise to these two DTA peaks are discussed below.

Infrared spectroscopy (IR)

Infrared spectra in the region 3000–4000 cm^{-1} of K^+-, Li^+-, and Al^{3+}-nontronite samples at ambient humidity and after dehydration at 200 and 300°C are shown in Figure 2. For K^+- and Li^+-nontronite, dehydration at 200°C totally removed the broad band centered at 3400 cm^{-1} that is characteristic of adsorbed water. The band at 3600 cm^{-1}, due to the vibrations of structural-OH groups, was only slightly reduced in intensity at 200°C. At 300°C, the intensity of this band was reduced significantly for all the samples. For the Li^+-nontronite sample, a band was present at 3270 cm^{-1} after dehydration.

In the region 1500–2000 cm^{-1} (Figure 3) the three exchange forms gave different spectra. The band due to the deformational vibration of adsorbed water at about 1600 cm^{-1} was absent for the K^+- and Al^{3+}-nontronites dehydrated at 200°C. In the Li^+-nontronite

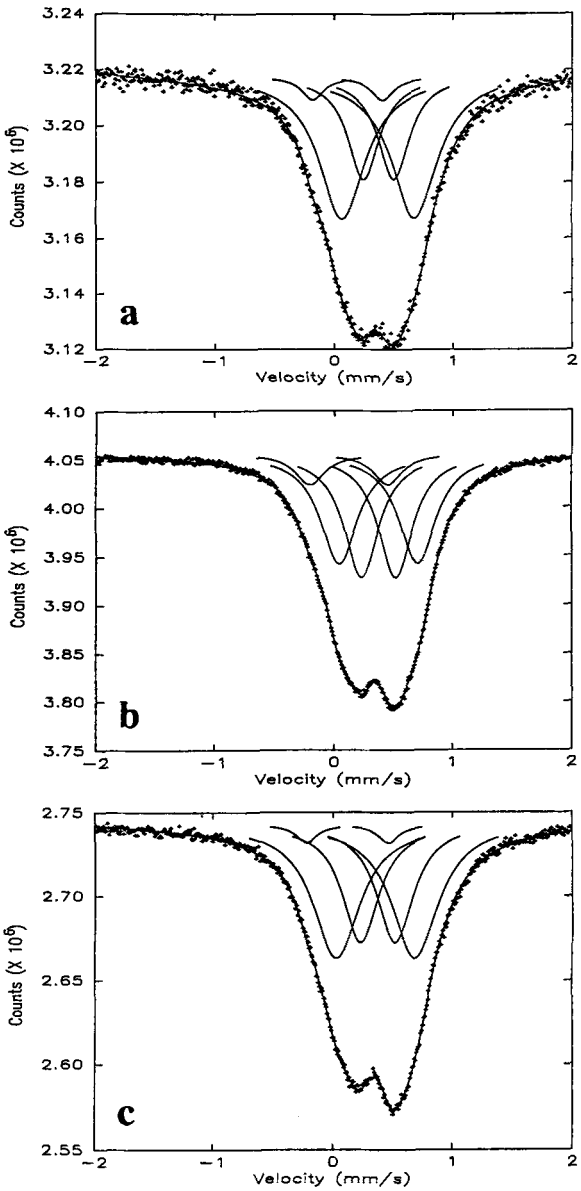


Figure 4. Room-temperature, computer-fitted Mössbauer spectra of K^+-nontronite at (a) ambient humidity, (b) heated at 200°C, and (c) heated at 300°C.

https://doi.org/10.1346/CCMN.1991.0390503 Published online by Cambridge University Press

https://doi.org/10.1346/CCMN.1991.0390503 Published online by Cambridge University Press

Table 1. Room-temperature, computer fitted Mössbauer parameters for nontronite samples containing different exchangeable cations and in various states of hydration.

	$^{VI}Fe^{3+}_{OUTER}$				$^{VI}Fe^{3+}_{INNER}$				$^{IV}Fe^{3+}$					
Cation[1]	IS (mm/s)	QS (mm/s)	W (mm/s)	A (%)	IS (mm/s)	QS (mm/s)	W (mm/s)	A (%)	IS (mm/s)	QS (mm/s)	W (mm/s)	A (%)	χ^2	MISFIT
K^+	0.37	0.61	0.47	64	0.37	0.25	0.32	32	0.11	0.59	0.22	5	593	$(3.1 \pm 0.7) \times 10^{-4}$
1LH[2]	(0.005)	(0.03)	(0.01)	(7)	(0.002)	(0.02)	(0.03)	(7)	(0.01)	(0.01)	(0.05)	(2)		
K^+	0.37	0.67	0.39	44	0.38	0.29	0.36	46	0.13	0.66	0.29	9.3	672	$(1.1 \pm 0.2) \times 10^{-4}$
200°C	(0.002)	(0.009)	(0.008)	(3)	(0.001)	(0.008)	(0.01)	(3)	(0.005)	(0.007)	(0.01)	(0.7)		
K^+	0.35	0.64	0.47	57	0.37	0.28	0.37	40	0.12	0.66	0.20	3.3	645	$(1.4 \pm 0.2) \times 10^{-9}$
300°C	(0.003)	(0.02)	(0.008)	(6)	(0.001)	(0.007)	(0.01)	(3)	(0.02)	(0.03)	(0.02)	(0.3)		
K^+	0.42	1.22	0.53	38	0.37	0.55	0.59	53	0.16	1.33	0.39	9	780	$(4.2 \pm 0.5) \times 10^{-4}$
400°C	(0.005)	(0.02)	(0.02)	(4)	(0.002)	(0.02)	(0.02)	(4)	(0.01)	(0.02)	(0.03)	(1)		
Na^+	0.38	0.64	0.36	33	0.37	0.29	0.35	55	0.17	0.53	0.28	11	596	$(1.9 \pm 0.4) \times 10^{-4}$
2LH[3]	(0.01)	(0.03)	(0.02)	(6)	(0.005)	(0.02)	(0.02)	(8)	(0.01)	(0.01)	(0.03)	(4)		
Na^+	0.40	0.62	0.32	29	0.39	0.29	0.37	54	0.20	0.56	0.30	17	618	$(1.2 \pm 0.2) \times 10^{-4}$
1LH	(0.005)	(0.02)	(0.01)	(4)	(0.001)	(0.01)	(0.01)	(5)	(0.007)	(0.01)	(0.01)	(2)		
Li^+	0.37	0.64	0.37	40	0.37	0.29	0.37	53	0.16	0.59	0.27	9	568	$(0.4 \pm 0.1) \times 10^{-4}$
1LH	(0.004)	(0.02)	(0.01)	(4)	(0.001)	(0.01)	(0.01)	(5)	(0.006)	(0.009)	(0.02)	(1)		
Li^+	0.37	0.75	0.39	32	0.37	0.37	0.38	64	0.07	0.80	0.24	4.4	695	$(2.1 \pm 0.3) \times 10^{-4}$
200°C	(0.002)	(0.02)	(0.01)	(4)	(0.001)	(0.008)	(0.01)	(4)	(0.008)	(0.01)	(0.02)	(1)		
Li^+	0.36	0.66	0.48	51	0.36	0.30	0.36	47	0.02	0.93	0.26	2.8	729	$(1.3 \pm 0.2) \times 10^{-4}$
300°C	(0.001)	(0.01)	(0.007)	(3)	(0.001)	(0.007)	(0.01)	(3)	(0.02)	(0.03)	(0.02)	(0.3)		
Ca^{2+}	0.34	0.23	0.33	40	0.35	0.60	0.42	55	0.20	0.67	0.20	4.7	596	$(1.1 \pm 0.2) \times 10^{-4}$
2LH	(0.01)	(0.01)	(0.02)	(5)	(0.01)	(0.02)	(0.01)	(5)	(0.01)	(0.01)	(0.01)	(0.5)		
Ca^{2+}	0.36	0.31	0.39	61	0.36	0.71	0.42	34	0.04	0.88	0.33	4.5	680	$(1.3 \pm 0.2) \times 10^{-4}$
1LH	(0.01)	(0.01)	(0.02)	(4)	(0.01)	(0.02)	(0.01)	(4)	(0.02)	(0.04)	(0.03)	(0.4)		
Ca^{2+}	0.36	0.33	0.40	58	0.36	0.73	0.46	38	0.00	0.95	0.29	4.3	692	$(1.5 \pm 0.2) \times 10^{-4}$
200°C	(0.01)	(0.01)	(0.01)	(4)	(0.01)	(0.02)	(0.01)	(3)	(0.01)	(0.01)	(0.02)	(0.2)		
Ca^{2+}	0.37	0.63	0.43	49	0.36	0.28	0.34	45	0.16	0.57	0.27	6	560	$(9 \pm 3) \times 10^{-4}$
R_{200}[4]	(0.01)	(0.03)	(0.01)	(6)	(0.003)	(0.01)	(0.02)	(8)	(0.02)	(0.02)	(0.05)	(3)		
Ca^{2+}	0.36	0.33	0.39	47	0.37	0.74	0.52	47	−0.02	1.00	0.31	5.3	697	$(0.8 \pm 0.1) \times 10^{-4}$
300°C	(0.01)	(0.01)	(0.01)	(2)	(0.01)	(0.01)	(0.01)	(3)	(0.01)	(0.01)	(0.02)	(0.2)		
Mg^{2+}	0.37	0.62	0.41	50	0.37	0.27	0.33	43	0.14	0.57	0.27	8	576	

https://doi.org/10.1346/CCMN.1991.0390503 Published online by Cambridge University Press

Table 1. Continued.

Cation[1]	$^{VI}Fe^{3+}_{OUTER}$ IS (mm/s)	QS (mm/s)	W (mm/s)	A (%)	$^{VI}Fe^{3+}_{INNER}$ IS (mm/s)	QS (mm/s)	W (mm/s)	A (%)	$^{IV}Fe^{3+}$ IS (mm/s)	QS (mm/s)	W (mm/s)	A (%)	χ^2	MISFIT
2LH	(0.005)	(0.02)	(0.009)	(5)	(0.002)	(0.01)	(0.02)	(5)	(0.009)	(0.01)	(0.03)	(2)		$(0.8 \pm 0.2) \times 10^{-4}$
Mg^{2+}	0.36	0.71	0.63	61	0.38	0.37	0.39	37	−0.12	1.20	0.14	2	974	
200°C	(0.001)	(0.02)	(0.006)	(4)	(0.001)	(0.008)	(0.01)	(4)	(0.004)	(0.008)	(0.01)	(0.1)		$(3.1 \pm 0.3) \times 10^{-4}$
Mg^{2+}	0.39	1.04	0.62	40	0.36	0.46	0.49	55	0.03	1.38	0.37	5.7	841	
300°C	(0.002)	(0.01)	(0.02)	(3)	(0.001)	(0.008)	(0.009)	(3)	(0.008)	(0.02)	(0.02)	(0.4)		$(3.1 \pm 0.3) \times 10^{-4}$
Fe^{3+}	0.37	0.63	0.43	46	0.37	0.24	0.38	52	0.20	0.70	0.19	3	608	
2LH	(0.003)	(0.02)	(0.01)	(4)	(0.001)	(0.006)	(0.03)	(3)	(0.005)	(0.01)	(0.03)	(1)		$(0.7 \pm 0.1) \times 10^{-4}$
Fe^{3+}	0.35	0.65	0.49	56	0.36	0.27	0.34	41	0.22	1.50	0.30	2.3	729	
200°C	(0.001)	(0.01)	(0.01)	(4)	(0.001)	(0.006)	(0.03)	(3)	(0.01)	(0.02)	(0.04)	(0.4)		$(1.7 \pm 0.2) \times 10^{-4}$
Fe^{3+}	0.38	0.81	0.59	43	0.40	0.33	0.49	51	0.20	1.59	0.63	6	567	
300°C	(0.002)	(0.02)	(0.03)	(5)	(0.001)	(0.01)	(0.02)	(5)	(0.02)	(0.02)	(0.05)	(1)		$(2.6 \pm 0.7) \times 10^{-5}$
Al^{3+}	0.38	0.62	0.35	37	0.36	0.28	0.33	51	0.16	0.51	0.29	12	595	
2LH	(0.006)	(0.02)	(0.009)	(3)	(0.003)	(0.008)	(0.01)	(4)	(0.009)	(0.007)	(0.02)	(3)		$(0.9 \pm 0.2) \times 10^{-4}$
Al^{3+}	0.35	0.68	0.52	69	0.36	0.29	0.32	30	0.17	1.79	0.36	1.4	695	
200°C	(0.001)	(0.01)	(0.007)	(3)	(0.001)	(0.005)	(0.01)	(2)	(0.02)	(0.04)	(0.07)	(0.3)		$(1.3 \pm 0.2) \times 10^{-4}$
Al^{3+}	0.36	0.78	0.67	80	0.35	0.32	0.34	18	0.25	1.82	0.38	3	628	
300°C	(0.001)	(0.03)	(0.02)	(6)	(0.002)	(0.01)	(0.03)	(5)	(0.02)	(0.04)	(0.09)	(1)		$(3.2 \pm 0.6) \times 10^{-4}$
Al^{3+}	0.41	0.74	0.55	50	0.37	0.35	0.37	31	0.20	0.62	0.47	18	635	
R_{300}[5]	(0.06)	(0.1)	(0.01)	(4)	(0.008)	(0.02)	(0.05)	(20)	(0.04)	(0.02)	(0.05)	(22)		$(2.0 \pm 0.4) \times 10^{-4}$

[1] Exchangeable cation present in Washington nontronite samples.
[2] 1-layer hydrate.
[3] 2-layer hydrate.
[4] Sample allowed to rehydrate in the atmosphere after heating at 200°C.
[5] Sample allowed to rehydrate in the atmosphere after heating at 300°C.

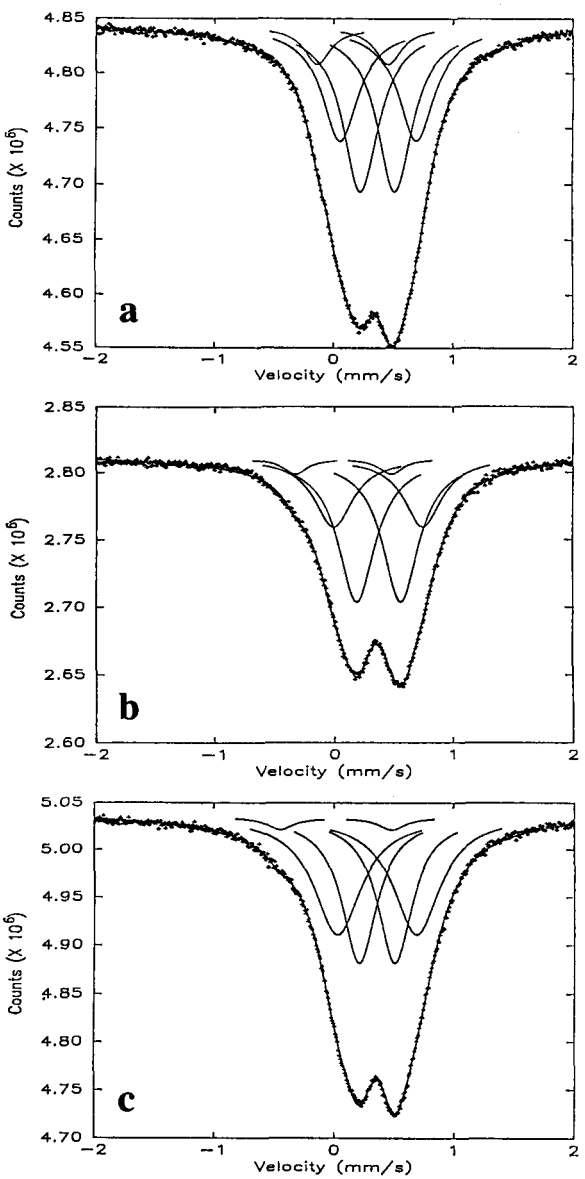


Figure 5. Room-temperature, computer-fitted Mössbauer spectra of Li^+-nontronite at (a) ambient humidity, (b) heated at 200°C, and (c) heated at 300°C.

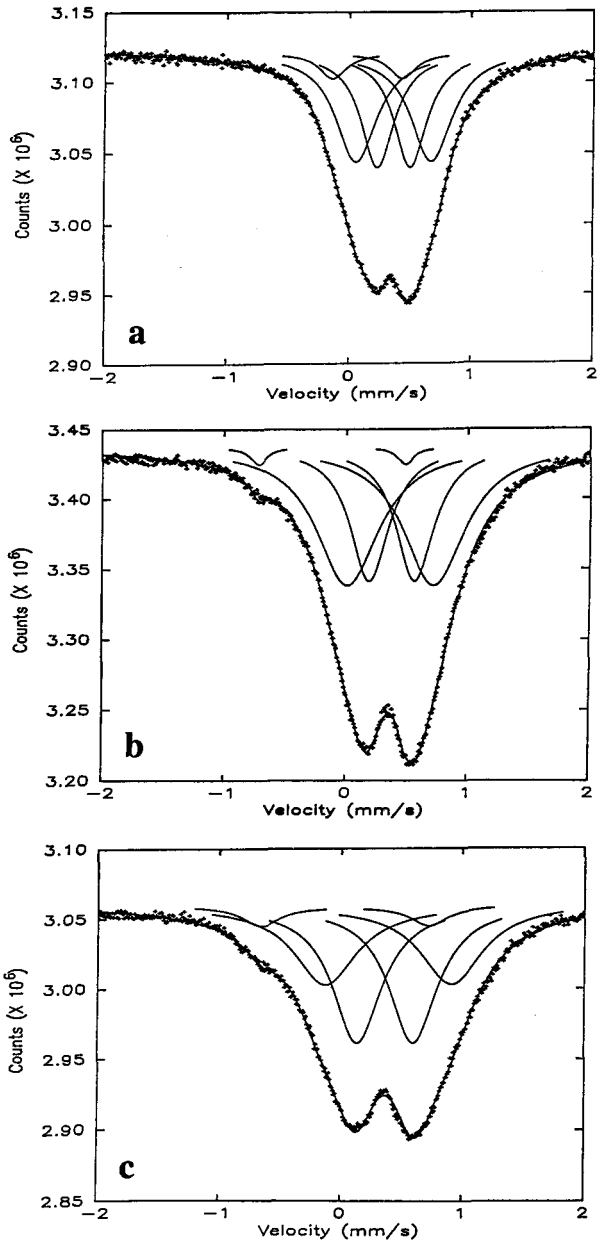


Figure 6. Room-temperature, computer-fitted Mössbauer spectra of Mg^{2+}-nontronite at (a) ambient humidity, (b) heated at 200°C, and (c) heated at 300°C.

two bands remained after dehydrating at 300°C, although the intensities of these bands were reduced.

Mössbauer spectra of hydrated nontronite samples

The RT Mössbauer spectra of cation-exchanged nontronite samples at ambient humidity are qualitatively similar (Figures 4a–8a). The width of the Mössbauer spectral envelope (W_m) has been approximated using the one-doublet computer fits. The width of the Mössbauer envelope for the samples at ambient humidity tended to decrease as the ionic potential (IP) of the exchangeable cations increased (Figure 9).

Mössbauer spectra of all of the samples were fitted using a three-doublet model representing Fe^{3+} in *cis*-octahedral sites and one tetrahedral site, in accordance with standard practice (Goodman *et al.*, 1976; Dainyak *et al.*, 1984; Johnston and Cardile, 1985 Dainyak and Drits, 1987). The line widths of the two *cis*-$^{VI}Fe^{3+}$ doublets were similar to those expected for discrete Fe^{3+} sites in silicate minerals (Bancroft, 1973). Progressive decrease in W_m on going from the K^+ to the Al^{3+} cation-exchanged form was reflected in the relative intensity

https://doi.org/10.1346/CCMN.1991.0390503 Published online by Cambridge University Press

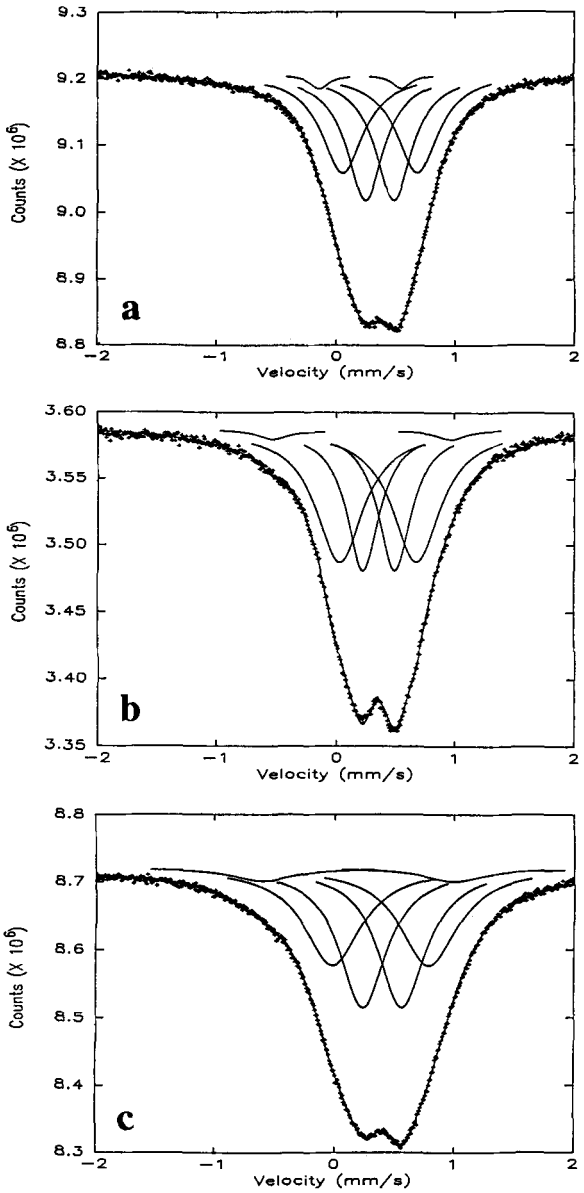


Figure 7. Room-temperature, computer-fitted Mössbauer spectra of Fe^{3+}-nontronite at (a) ambient humidity, (b) heated at 200°C, and (c) heated at 300°C.

of the outer- and inner-*cis* octahedral Fe^{3+} doublets ($^{VI}Fe^{3+}_{OUTER}$ and $^{VI}Fe^{3+}_{INNER}$).

The ratio of the intensities of the $^{VI}Fe^{3+}_{OUTER}$ and $^{VI}Fe^{3+}_{INNER}$ doublets (R_{MOSS}) is plotted in Figure 10 vs the ionic potential of the exchangeable cation for 1-layer and 2-layer hydrates. For the 2-layer hydrates (obtained at ambient humidity for Ca^{2+}-, Mg^{2+}-, Fe^{3+}-, and Al^{3+}-exchanged nontronite samples) a linear relationship was obtained between R_{MOSS} and IP, and was also suggested for the 1-layer hydrates (obtained at ambient humidity for Cs^{+}-, K^{+}-, Na^{+}-, and Li^{+}-ex-

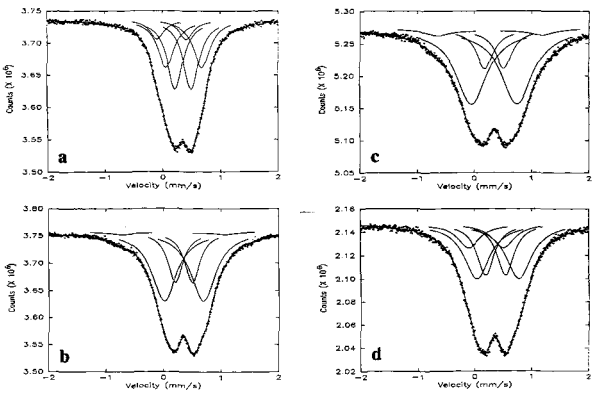


Figure 8. Room-temperature, computer-fitted Mössbauer spectra of Al^{3+}-nontronite at (a) ambient humidity, (b) heated at 200°C, (c) heated at 300°C, and (d) sample from (c) exposed to the atmosphere.

changed nontronite samples). Here, however, the data points were considerably more scattered.

Mössbauer spectra of dehydrated nontronite samples

With the exception of the K^{+}- and Na^{+}-nontronite, Mössbauer spectra of the cation-exchanged nontronite samples dehydrated at 200 and 300°C exhibited shoulders at about −0.5 mm/s (Figures 5b, 5c, 6b, 6c, 7b, 7c, 8b, 8c). In addition to fitting two $^{VI}Fe^{3+}$ doublets to these spectra, doublets with parameters appropriate to Fe^{3+} in tetrahedral sites of phyllosilicates ($^{IV}Fe^{3+}$) had to be included in the fitting model for the fits to be satisfactory. The isomer shift (IS) of these $^{IV}Fe^{3+}$ doublets was ≤0.25 mm/s, and the QS value was variable. Parameters are given in Table 1.

Spectra of the dehydrated samples fitted with three-doublet models gave poorer fitting statistics for almost all samples studied than did spectra of the correspond-

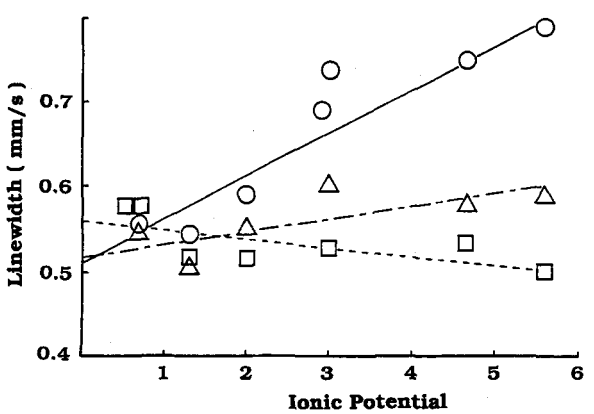


Figure 9. Relationship between Mössbauer spectral line width, as measured by a one-doublet computer fit (W_m), and the ionic potential of the exchangeable cations (IP) for samples at ambient relative humidity (squares), dehydrated at 200°C (triangles), and dehydrated at 300°C (circles).

https://doi.org/10.1346/CCMN.1991.0390503 Published online by Cambridge University Press

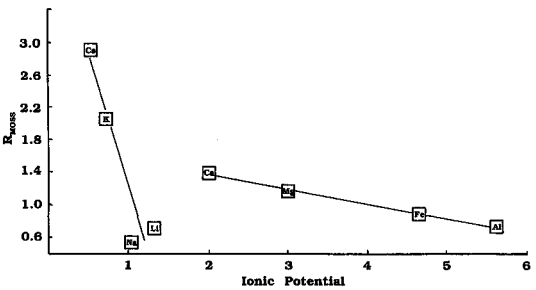


Figure 10. Relationship between ratio of outer- and inner-$^{VI}Fe^{3+}$ doublets (R_{MOSS}) and ionic potential of exchangeable cations (IP) for nontronites at ambient humidity. Cs^+, K^+, Na^+, and Li^+ form 1-layer hydrates, whereas Ca^{2+}, Mg^{2+}, Fe^{3+}, and Al^{3+} form 2-layer hydrates.

ing hydrated samples. For example, the spectrum of the 2-layer hydrate of Mg^{2+}-nontronite fitted with a three-doublet model gave $\chi^2 = 576$, whereas the spectrum of the same sample dehydrated at 200°C gave $\chi^2 = 974$. Although this latter fit may seem unsatisfactory, it is nonetheless a significant improvement over the fit obtained using a two-$^{VI}Fe^{3+}$ doublet model which gave $\chi^2 = 1611$. For all dehydrated nontronite samples the three-doublet models gave vastly improved fits over the two-doublet models. Poorer χ^2 values for the dehydrated samples are therefore probably indicative of increasing structural disorder that is also suggested by the broadening of XRD reflections.

A plot of QS for the $^{IV}Fe^{3+}$ doublet vs the IP of the exchangeable cations after dehydration at 200°C shows that the QS value increases as IP increases (Figure 11b). Dehydration at 300°C (Figure 11c) resulted in QS values for the $^{IV}Fe^{3+}$ doublet that were very close to those obtained at 200°C. The QS value of the $^{VI}Fe^{3+}_{OUTER}$ doublet for the three samples containing exchangeable cations with the highest IP was somewhat larger at 300°C than at 200°C, but it was comparable for samples containing exchangeable cations of lower IP. The QS value of the $^{VI}Fe^{3+}$ doublets was not affected as dramatically as the $^{IV}Fe^{3+}$ doublets, but their relative areas changed noticeably upon dehydration.

A plot of R_{MOSS} against IP of the exchangeable cation for samples dehydrated at 200°C is shown in Figure 12. As the IP of the exchangeable cation increased the intensity of the $^{VI}Fe^{3+}_{OUTER}$ doublet increased relative to that of the $^{IV}Fe^{3+}_{INNER}$ doublet. Therefore, the number of the more distorted Fe^{3+}-containing octahedra increased as the IP of the migrating exchangeable cation increased. At 300°C, no relationship was apparent between the exchangeable cation and the ratio of the areas of the two $^{VI}Fe^{3+}$ doublets, probably because of disorder about the octahedral cation sites arising from partial deprotonation of the structural hydroxyl groups, and possibly partial dehydroxylation.

At 200°C W_m increased only slightly as the IP of the exchangeable cations increased (Figure 9). However,

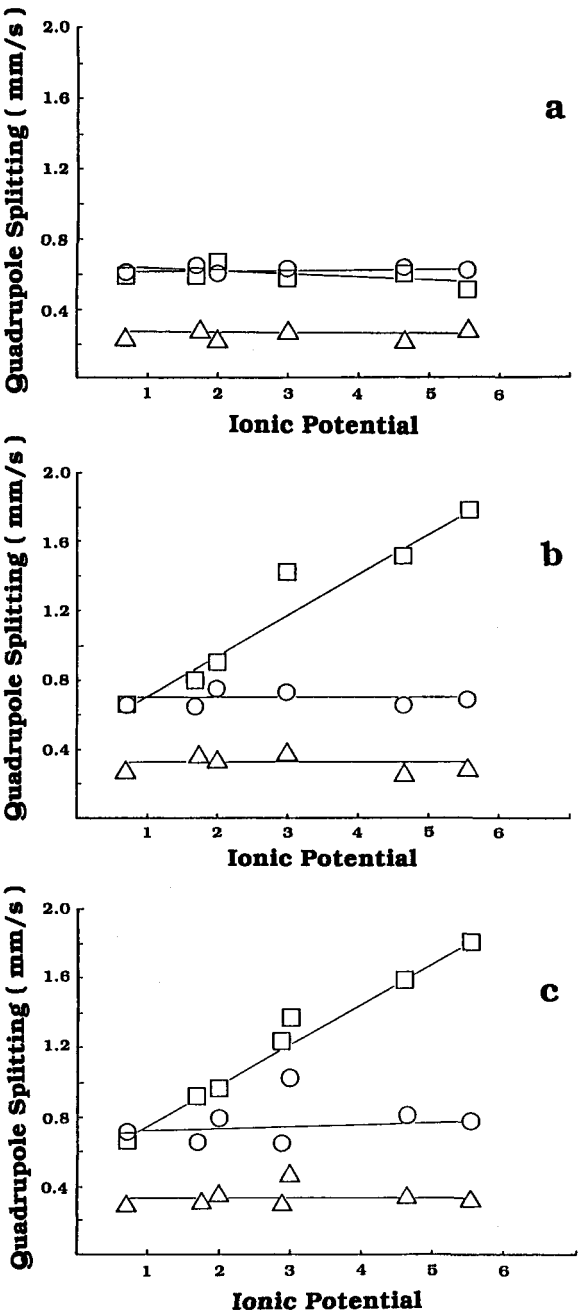


Figure 11. Relationship between quadrupole splitting (QS) of three Mössbauer doublets and ionic potential (IP) of exchangeable cations at (a) ambient humidity, (b) after dehydration at 200°C, and (c) dehydration at 300°C (circles = $^{VI}Fe^{3+}_{OUTER}$, triangles = $^{VI}Fe^{3+}_{INNER}$, squares = $^{IV}Fe^{3+}$).

at 300°C, W_m increased sharply as IP of the exchangeable cation increased. This trend was the reverse of that observed in the spectra of the samples at ambient humidity. The K^+-nontronite was unaffected by dehydration at 300°C, although heating to 400°C resulted in a marked increase in W_m, presumably due to the

https://doi.org/10.1346/CCMN.1991.0390503 Published online by Cambridge University Press

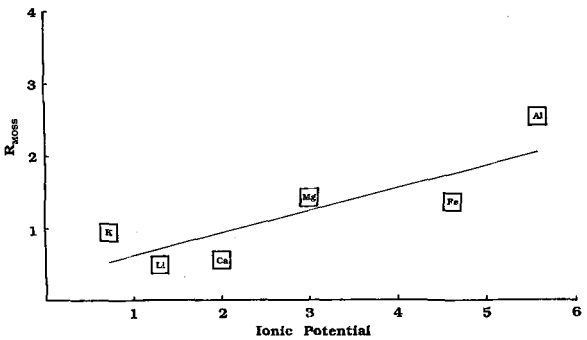


Figure 12. Relationship between ratio of outer- and inner-$^{VI}Fe^{3+}$ doublets (R_{MOSS}) and ionic potential of exchangeable cations (IP) for nontronites dehydrated at 200°C.

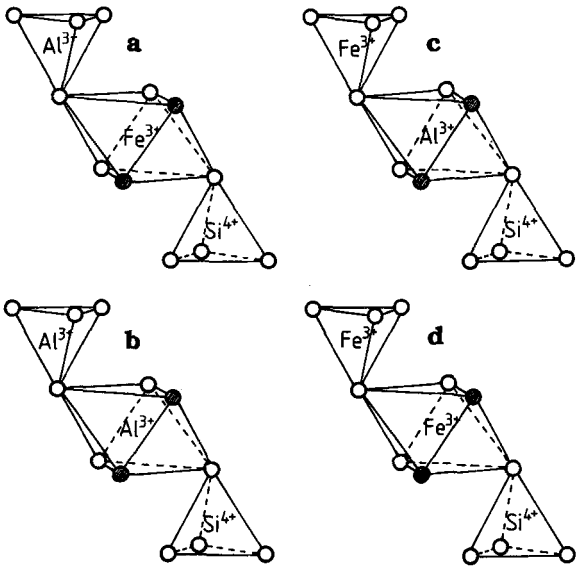


Figure 13. Substitutional variants in reduced structural unit of nontronite.

onset of dehydroxylation. Only heating to 400°C resulted in Mössbauer parameters indicating possible dehydroxylation by the formation of five-coordinate Fe^{3+} sites (e.g., Heller-Kallai and Rozenson, 1980). Thus, the dehydration temperature used in the present work never exceeded 300°C.

Changes in IS of the $^{IV}Fe^{3+}$ sites after heating also depended on the exchangeable cations. For the Li^+-, Ca^{2+}-, and Mg^{2+}-nontronite samples the IS of $^{IV}Fe^{3+}$ sites decreased on heating the sample. In contrast, IS increased after heating the Al^{3+}-nontronite and did not change after heating the Fe^{3+}-nontronite.

Mössbauer spectra of rehydrated samples

The Mössbauer spectrum of Ca^{2+}-nontronite dehydrated at 200°C, and then exposed to the atmosphere so that the interlayers rehydrated with two water layers (d(001) = 14.7 Å), was similar to the spectrum of samples at ambient humidity. The low-velocity shoulder was absent, and QS and IS values of the $^{IV}Fe^{3+}$ sites were about the same as in the samples at ambient humidities. The intensity of the $^{VI}Fe^{3+}_{OUTER}$ doublet increased after rehydration, but did not quite reach the value it had at 200°C, although the QS value for this site was almost completely restored. Spectra for the Ca^{2+}-exchanged samples are given in Luca and Cardile (1989), and parameters are given in Table 1.

The Al^{3+}-nontronite also displayed some reversibility after dehydration at 300°C, as is shown by the computer-fitted spectrum of the rehydrated sample (Figure 8d). Here QS and IS of the $^{IV}Fe^{3+}$ sites were almost completely restored to their values at ambient humidity, but the QS and the intensity of the $^{VI}Fe^{3+}$ doublets were only partly restored.

DISCUSSION

A shoulder developed at about −0.5 mm/s in the Mössbauer spectra of dehydrated nontronite samples containing exchangeable cations with ionic potentials greater than, or equal to that of Li^+. To fit spectra containing such shoulders, a doublet with IS < 0.30 mm/s, but variable QS, had to be included in the fitting model that initially contained only two intense $^{VI}Fe^{3+}$ doublets. Trivalent Fe in the tetrahedral sheets of micas and clay minerals usually has IS = 0–0.30 mm/s, and more variable QS (Annersten and Olesch, 1978; Pavlishin *et al.*, 1978; Sanz *et al.*, 1978; Coey *et al.*, 1984; Dyar and Burns, 1986; Cardile and Slade, 1987; Dyar, 1987; Ferrow, 1987). The doublets responsible for the shoulders at low velocity in the spectra of the dehydrated cation-exchanged nontronite samples all have IS values in this range. They are, therefore, probably due to Fe^{3+} in the tetrahedral sheet. A similar proposal was made by Luca (1991) for the appearance of similar doublets in the Mössbauer spectra of dehydrated Ca^{2+}-exchanged nontronite samples. The following main arguments were given for this assignment: (1) the appearance of the shoulder is dependent on the type of exchangeable cation, and cation-exchange capacity is a property of nontronite; (2) ostensibly pure nontronite samples known to contain considerable tetrahedral Fe^{3+} produce a similar shoulder on Ca^{2+}-exchange and dehydration.

Radoslovich and Norrish (1962) suggested that the tetrahedra of 2:1 layer silicates rotate freely. Moreover, Leonard and Weed (1967) and Lahav and Bresler (1973) demonstrated that the type and hydration state of the exchangeable cations affects tetrahedral sheet rotation, which in turn influences the *b*-dimension of the octahedral sheet. In the present study, increasing QS values for the $^{IV}Fe^{3+}$ sites as the IP of the exchangeable cation increases shows that exchangeable cations with higher IP distort the $^{IV}Fe^{3+}$ sites more.

Insensitivity of the QS value of the $^{IV}Fe^{3+}$ doublet to hydration state in the K^+- and Na^+-nontronite sam-

https://doi.org/10.1346/CCMN.1991.0390503 Published online by Cambridge University Press

ple is consistent with these cations maintaining a fixed position relative to $^{IV}Fe^{3+}$ in all hydration states. This is similar to the findings of Low (1981) that exchangeable Na^+ cations remain closely associated with montmorillonite layers, regardless of the amount of interlayer water. In contrast, the sensitivity of QS values of $^{IV}Fe^{3+}$ sites to changes in hydration state (in the case of samples containing exchangeable cations with IP greater than Li^+) implies that these cations move toward $^{IV}Fe^{3+}$ sites as water is removed. The suggestion that exchangeable cations become coordinated to AlO_4 tetrahedra of phyllosilicates has been made previously by Radoslovich and Norrish (1962) and Leonard and Weed (1967). Moreover, for exchangeable cations with IP greater than that of Li^+ the changes in Mössbauer parameters of the $^{IV}Fe^{3+}$ sites after dehydration can be reversed by rehydration. This further reinforces the view that exchangeable cations with IP greater than, or equal to Li^+ change their position with respect to the basal surfaces as the hydration state of the nontronite changes.

To explain the similar layer stacking disorder of nontronite and montmorillonite during dehydration, Suquet *et al.* (1987) hypothesized that, like montmorillonite, dehydration of nontronite results in the movement of exchangeable cations into the pseudohexagonal cavities. Although the layer charge in nontronite originates predominantly in the tetrahedral sheet, as in beidellite, the charge was considered by Suquet *et al.* (1987) to be nevertheless at least partially localized on structural OH groups at the bottom of the pseudohexagonal cavities. The reason given for this was that if an $^{IV}Al^{3+}$ site is adjacent to an octahedron containing a more electronegative cation, such as Fe^{3+} (Figure 13a), the layer charge would be localized on the $FeO_4(OH)_2$ octahedron, and not on the $^{IV}Al^{3+}$ site. Conversely, if the $^{IV}Al^{3+}$ site is adjacent to an $^{VI}Al^{3+}$ site (Figure 13b), the negative charge would be localized on the oxygen atoms of the $^{IV}Al^{3+}$ site. Only $^{IV}Al^{3+}$-$^{IV}Si^{4+}$ substitution was considered by Suquet *et al.* (1987) because the presence of $^{IV}Fe^{3+}$ sites was thought to be minimal.

If significant $^{IV}Fe^{3+}$ is present, the arguments of Suquet *et al.* (1987) can be extended by considering the remaining substitutional variants shown in Figures 13c and 13d. In the situation depicted in Figure 13c, the electronegativity of the Fe^{3+} cation in the tetrahedron is probably greater than that of Al^{3+} in the octahedron. Therefore, the charge created by the $^{IV}Fe^{3+}$-$^{IV}Si^{4+}$ substitution should be localized essentially on the oxygen atoms of the $^{IV}Fe^{3+}$ site. The effect of retaining octahedral sites containing Fe^{3+} with layer charge created by $^{IV}Fe^{3+}$-$^{IV}Si^{4+}$ substitutions (Figure 13d) is again the localization of charge on the $^{IV}Fe^{3+}$ site because a greater electronegativity is expected for the $^{IV}Fe^{3+}$ site than for the $^{VI}Fe^{3+}$ site (Brown, 1981). The ability of a sample containing a high proportion of $^{IV}Fe^{3+}$ sites to produce ordered layer stacking over a wide range of relative humidities is expected to be greater than a sample containing little or no $^{IV}Fe^{3+}$. Because negative charge is expected to be localized on the Fe^{3+}-containing tetrahedron, exchangeable cations may be located above these tetrahedra. Inasmuch as each of the four substitutional variants given in Figure 13 is expected to be present in SWa-1 nontronite, exchangeable cations should migrate toward tetrahedral and octahedral Fe^{3+} sites, thus influencing the Mössbauer parameters of these sites. This is what is observed experimentally (Figure 11). The greater sensitivity of the $^{IV}Fe^{3+}$ sites to changes in interlayer structure is consistent with the notion that the tetrahedral sheet is more flexible than the octahedral sheet, implying that greater bond length and angle changes would result in the tetrahedral sheet during dehydration. In this regard, parallel experiments on nontronite deriving all layer charge from $^{IV}Fe^{3+}$-$^{IV}Si^{3+}$ substitutions, and nontronite deriving all layer charge from $^{IV}Al^{3+}$-$^{IV}Si^{4+}$ would be of interest.

The present results show that at 200°C the intensity of the $^{VI}Fe^{3+}_{OUTER}$ doublet corresponding to the more distorted *cis*-octahedral sites increased as the IP of the exchangeable cations increased. Many factors may have contributed to an increase in the number of more distorted $^{IV}Fe^{3+}$ sites during dehydration, including: 1. direct electronic interaction of exchangeable cations within the pseudohexagonal cavities; 2. changes in the orientation of the structural OH groups at the bottom of the pseudohexagonal cavities; 3. changes in the dimensions of the octahedral sheet induced by the interaction of exchangeable cations with tetrahedral sites, as discussed above; and 4. changes in the layer stacking order-disorder.

The ability of cations with high IP to distort and destabilize the nontronite structure during dehydration is reinforced by both DTA and IR results. The DTA results show that the dehydroxylation temperature is lowest for exchangeable cations of high IP. Infrared results also demonstrate that exchangeable cations of high IP are more reactive during dehydration.

Reduction in the intensity of the OH-stretching vibrations after the nontronite samples were heated to 200°C were probably not due to dehydroxylation since TGA and DTA results indicated that this does not occur until at least 400°C. Instead, it is possible that proton delocalization is occurring at 200–300°C, as has been observed on a number of aluminosilicate minerals in this temperature range (Fripiat *et al.*, 1967), and in kaolinites (Fripiat and Toussaint, 1963; Maiti and Freund, 1981). Furthermore, heating the nontronite films to 300°C under vacuum caused them to turn a dark, blue-black color, whereas nontronite samples heated in air were orange. It is possible that removal of OH protons without dehydroxylation occurring causes reduction of the octahedral Fe^{3+} cations, which changes the color of the clay. Partial reduction of structural Fe^{3+} cations has been observed after heating vermiculite (Drago *et al.*, 1977) and montmorillonite

https://doi.org/10.1346/CCMN.1991.0390503 Published online by Cambridge University Press

(Plachinda *et al.*, 1972). The Mössbauer spectrum of Al^{3+}-nontronite heated at 300°C under vacuum exhibited a small Fe^{2+} resonance, indicating that partial reduction of structural Fe^{3+} had occurred.

Bands at 3400 cm^{-1} remaining in the IR spectrum of the Al^{3+}-nontronite after heating to 200 and 300°C (Figure 2c) could not have been due to adsorbed water, because even at 200°C the OH-bending vibrations of adsorbed water were absent. Proton attack of Si-O-Al linkages to produce Si-OH-Al groups occurs in decationated NH_4^+-beidellite (Plee *et al.*, 1985) and pillared beidellite (Poncelet and Schutz, 1986), and these OH groups vibrate at 3400 cm^{-1}. Dehydration of Al^{3+}-nontronite should also produce sufficient acidity to promote proton attack of Si-O-Al groups in this nontronite. The bands at 3400 cm^{-1} in the IR spectrum of the dehydrated Al^{3+}-nontronite samples are therefore assigned to Si-OH-Al groups of adjacent tetrahedra.

The behavior of the Li^+-nontronite during dehydration was anomalous. Only in this sample were IR bands present at 3270 cm^{-1} and 1600 cm^{-1}, and an unusual DTA trace was observed. The band at 3270 cm^{-1} in the dehydrated samples (Figure 2b(ii)) must be the corresponding OH-stretching vibration of water trapped in the pseudohexagonal cavities when the interlayers collapse. A similar observation has been made for Li^+-saponite using IR spectroscopy (Suquet *et al.*, 1982). The unusual DTA results are also consistent with this hypothesis. One of the endotherms at around 500°C probably arises from dehydroxylation and the loss of water trapped in the pseudohexagonal cavities, while the other is due to removal of structural hydroxyl groups. A requirement for being able to trap water in the pseudohexagonal cavities is a face-to-face arrangement of adjacent pseudohexagonal cavities. As a result, the layers of dehydrated Li^+-nontronite may be more ordered than the other dehydrated, cation-exchanged nontronites. This may explain why the dehydrated Li^+-nontronite gives a relatively intense and narrow (001) XRD reflection after heating to 200 and 300°C as compared with the other cation-exchanged nontronite samples. Nontronite samples exchanged with cations that are sufficiently small to penetrate into the pseudohexagonal cavities, but that do not remain coordinated to a water molecule, are characterized by very broad, diffuse (001) XRD reflections after dehydration. This signifies severe *c*-axis disorder in these systems.

SUMMARY AND CONCLUSIONS

The present study has demonstrated that the nontronite structure is sensitive to hydration state. All of the structural Fe^{3+} sites are affected to various degrees by dehydration, and consequent movement of the exchangeable cations toward the silicate layers influences the Mössbauer parameters of the $^{IV}Fe^{3+}$ sites most. If the nontronite contains exchangeable cations of high ionic potential, a pronounced shoulder develops at about −0.5 mm/s. The doublet required to adequately fit spectra containing such a shoulder has IS characteristic of $^{IV}Fe^{3+}$ sites in phyllosilicates.

The QS value of the $^{IV}Fe^{3+}$ sites increases linearly and steeply with the IP of the exchangeable cations after dehydration, indicating increasing distortion of the FeO_4 tetrahedral angles and bond lengths. This distortion occurs after only mild dehydration, such as a reduction in hydration state from a 2-layer hydrate to a 1-layer hydrate. Quadrupole splitting of the $^{VI}Fe^{3+}$ sites was not as sensitive to the position of the exchangeable cations relative to the silicate sheets.

The dehydration of nontronite may be divided into three temperature regimes, the boundaries being affected by the exchangeable cation. For Al^{3+}-exchanged nontronite, which has the greatest thermal lability of the nontronite samples studied, these temperature regimes may be defined as follows:

1. Room temperature–250°C. Removal of interlayer water and migration of exchangeable cations toward tetrahedral and octahedral sites on which negative charge is localized. At about 200°C, deprotonation of structural hydroxyl groups begins.

2. 250°C–450°C. Dehydroxylation of the nontronite structure.

3. >450°C. Irreversible structure breakdown and transformation into other phases.

An interesting picture of nontronite dehydration has been developed in which several processes operate. The role of exchangeable cations seems to be pivotal in many of these processes. Distortion of the nontronite structure appears to commence under very mild conditions.

ACKNOWLEDGMENTS

The author thanks Dr. J. H. Johnston (Victoria University, Wellington, New Zealand) for the use of Mössbauer facilities and the Solid State Chemistry Section, Chemistry Division, Department of Scientific and Industrial Research, New Zealand, for access to computing facilities.

REFERENCES

Annersten, A. and Olesch, M. (1978) Distribution of ferrous and ferric iron in clintonite and the Mössbauer characteristics of ferric iron in tetrahedral coordination: *Can. Mineral.* **16,** 199–203.

Badran, A. H., Dwyer, J., Evmiridis, N. P., and Manford, J. A. (1977) Ferric ion exchange and breakdown of crystalline structure in zeolites: *Inorganica Chimica Acta* **21,** 61–64.

Bancroft, G. M. (1973) *Mössbauer Spectroscopy: An Introduction for Inorganic Chemists and Geochemists:* McGraw-Hill, London, p. 32.

Brigatti, M. F. (1983) Relationships between composition and structure in Fe rich smectites: *Clay Miner.* **18,** 177–186.

https://doi.org/10.1346/CCMN.1991.0390503 Published online by Cambridge University Press

Brindley, G. W. and Kao, C. C. (1980) Formation, composition, and properties of hydroxy-Al and hydroxy-Mg-montmorillonite: *Clays & Clay Minerals* **28,** 435–443.

Brown, I. D. (1981) The bond-valence method: An empirical approach to chemical structure and bonding: in *Structure and Bonding in Crystals, Vol. II,* M. O'Keefe and A. Navrotsky, eds., Academic Press, New York, 1–30.

Cardile, C. M. (1985) Structural studies of selected smectites: Ph.D. thesis, Victoria University, Wellington, New Zealand, 205 pp.

Cardile, C. M. and Slade, P. G. (1987) Structural study of a benzidine-vermiculite intercalate having a high tetrahedral-iron content by ^{57}Fe Mössbauer spectroscopy: *Clays & Clay Minerals* **35,** 203–207.

Coey, J. M. D., Chukhrov, F. V., and Zvyagin, B. B. (1984) Cation distribution, Mössbauer spectra, and magnetic properties of ferripyrophyllite: *Clays & Clay Minerals* **32,** 198–204.

Dainyak, L. G., Bookin, A. S., and Drits, V. A. (1984) Interpretation of Mössbauer spectra of dioctahedral Fe^{3+} containing layer silicates. II. Nontronite: *Sov. Phys. Crystallogr.* **29,** 181–185.

Dainyak, L. G. and Drits, V. A. (1987) Interpretation of Mössbauer spectra of nontronite, celadonite, and glauconite: *Clays & Clay Minerals* **35,** 363–372.

Drago, V., Baggio-Saitovich, E., and Danon, J. J. (1977) Mössbauer spectroscopy of electron irradiated natural layer silicates: *J. Inorg. Nucl. Chem.* **39,** 973–979.

Dyar, M. D. (1987) A review of Mössbauer data on trioctahedral micas: Evidence for tetrahedral Fe^{3+} and cation ordering: *Amer. Mineral.* **72,** 102–112.

Dyar, M. D. and Burns, R. G. (1986) Mössbauer spectral study of ferruginous one-layer trioctahedral micas: *Amer. Mineral.* **71,** 955–965.

Ferrow, E. (1987) Mössbauer and X-ray studies on the oxidation of annite and ferriannite: *Phys. Chem. Miner.* **14,** 270–275.

Fripiat, J. J., Rouxhet, P. G., Jacobs, H., and Jelli, A. (1967) La delocalisation des protons dans les solides inorganiques: *Bull. Groupe Fr. Argiles* **19,** 87–95.

Fripiat, J. J. and Toussaint, F. (1963) Dehydroxylation of kaolinite. II. Conductometric measurements and infrared spectroscopy: *J. Phys. Chem.* **67,** 30–36.

Goodman, B. A., Russell, J. D., and Fraser, A. R. (1976) A Mössbauer and I. R. spectroscopic study of the structure of nontronite: *Clays & Clay Minerals* **24,** 54–59.

Heller-Kallai, L. and Rozenson, I. (1980) Dehydroxylation of dioctahedral phyllosilicates: *Clays & Clay Minerals* **28,** 355–368.

Johnston, J. H. and Cardile, C. M. (1985) Iron sites in nontronite and the effect of interlayer cations from Mössbauer spectra: *Clays & Clay Minerals* **33,** 21–30.

Lahav, N. and Bresler, E. (1973) Exchangeable cation-structural parameter relationships in montmorillonite: *Clays & Clay Minerals* **21,** 249–255.

Leonard, R. A. and Weed, S. B. (1967) Influence of exchange ions on the *b*-dimensions of dioctahedral vermiculite: *Clays & Clay Minerals* **15,** 149–161.

Low, P. F. (1981) The swelling of clay: III. Dissociation of exchangeable cations: *Soil Sci. Soc. Amer. J.* **45,** 1074–1078.

Luca, V. and Cardile, C. M. (1989) Improved detection of tetrahedral Fe^{3+} in nontronite SWa-1 through Mössbauer spectroscopy: *Clay Miner.* **24,** 115–119.

Luca, V. (1991) Detection of tetrahedral Fe^{3+} sites in nontronite and vermiculite by Mössbauer spectroscopy. *Clays & Clay Minerals* **39,** 467–477.

Maiti, G. C. and Freund, F. (1981) Dehydration related proton conductivity in kaolinite: *Clay Miner.* **16,** 395–413.

Pavlishin, V. I., Platonov, A. N., Polshin, E. V., Semenova, T. F., and Starova, G. L. (1978) Micas with iron in quadruple coordination: *Zapisky Vses. Mineral. Obshchestva* **107,** 165–176.

Plachinda, A. S., Ovcharenko, F. D., Makarov, E. F., Tarasevich, Yu. I., Baldokhin, Yu. V., and Suzdalev, I. P. (1972) Reduction of iron(III) to iron(II) during the heating of iron containing clay minerals in vacuo: *Dokl. Akad. Nauk. S.S.S.R.* **206,** 1373–1376.

Plee, D., Schutz, A., Poncelet, G., and Fripiat, J. J. (1985) Acid properties of bidimensional zeolite: in *Catalysis by Acids and Bases,* B. Imelik, C. Naccache, G. Coudurier, J. Ben Taarit, and J. C. Vedrine, eds., Elsevier, Amsterdam, 343–350.

Poncelet, G. and Schutz, A. (1986) Pillared montmorillonite and beidellite. Acidity and catalytic properties: in *Chemical Reactions in Organic and Inorganic Constrained Systems,* R. Setton, ed., Reidel, Dordrecht, 165–178.

Radoslovich, E. W. and Norrish, K. (1962) The cell dimensions and symmetry of layer-lattice silicates. I. Some structural considerations: *Amer. Mineral.* **47,** 599–616.

Sanz, J., Meyers, J., Vieloye, L., and Stone, W. E. E. (1978) The location of iron in natural biotites and phlogopites: A comparison of several methods: *Clay Miner.* **13,** 45–52.

Suquet, H., Malard, C., and Pezerat, H. (1987) Structure et proprietes d'hydratation des nontronites: *Clay Miner.* **22,** 157–167.

Suquet, H., Prost, R., and Pezerat, H. (1982) Etude par spectroscopie et diffraction × des interactions eau cation-feuliet dans les phases a 14.6, 12.2 et 10.2Å d'une saponite-Li de synthese: *Clay Miner.* **17,** 231–241.

(Received 31 May 1989; accepted 17 June 1991; Ms. 1914)

https://doi.org/10.1346/CCMN.1991.0390503 Published online by Cambridge University Press